Chemically Resistant, Electric Conductive, and Superhydrophobic Coatings

Saddiqi, Naeem-ul-Hasan ; Seeger, Stefan

Abstract: In this study, the fabrication of superhydrophobic and conductive coatings applying a facile coating method is reported. The droplet-assisted growth and shaping (DAGS) method is used to synthesize silicone nanofilament–based superhydrophobic coatings. Dip coating of superhydrophobic substrates in carbon nanofiber suspensions is performed to prepare superhydrophobic/conductive coatings. The prepared coatings combine electric conductivity, optical transparency, and superhydrophobicity with low sliding angles. The coatings show stability to water immersion and exposure to extreme humid conditions. Also, they exhibit good chemical resistance after several days of immersion in acidic and basic aqueous solutions. A key factor of such coatings is the mechanical durability which is improved by the addition of Parafilm-M

DOI: https://doi.org/10.1002/admi.201900041

Chemically Resistant, Electric Conductive & Superhydrophobic Coatings

*Naeem-ul-Hasan Saddiqi, Stefan Seeger**

Naeem-ul-Hasan Saddiqi, Prof. Dr. Stefan Seeger
Department of Chemistry, University of Zurich, Winterthurerstrasse 190, 8057 Zurich
E-mail: sseeger@chem.uzh.ch

Keywords: silicone nanofilaments, superhydrophobic coatings, droplet assisted growth and shaping, electrically conductive coatings, carbon nanofibers

In this study, the fabrication of superhydrophobic and conductive coatings applying a facile coating method is reported. The droplet assisted growth and shaping (DAGS) method is used to synthesize silicone nanofilament-based superhydrophobic coatings. Dip coating of superhydrophobic substrates in carbon nanofiber suspensions is performed to prepare superhydrophobic/conductive coatings. The prepared coatings combine electric conductivity, optical transparency, and superhydrophobicity with low sliding angles. The coatings show stability to water immersion and exposure to extreme humid conditions. Also, they exhibit good chemical resistance after several days of immersion in acidic and basic aqueous solutions. A key factor of such coatings is the mechanical durability which is improved by the addition of Parafilm-M.

1. Introduction

The superhydrophobic coatings inspired by objects in nature have gained considerable attention for various applications such as self-cleaning,[1][2][3][4] antifogging,[5][6] drag reduction,[7] anti-icing,[8] antireflective,[9][10] and oil/water separation.[11][12] In general, practicability, scalability and good chemical and mechanical stability of superhydrophobic coatings is required for their practical use, but multi-functionality of superhydrophobic coatings has been a new focus of academic and industrial interest. Thanks to such interest of

making superhydrophobic surfaces smarter by adding some functionalities, recent studies show fabrication of superhydrophobic surfaces with added functionalities such as optical transparency,[13] antimicrobial activity,[14] magnetism[15][16] and electrical conductivity etc.[17]

For example, superhydrophobic surfaces combined with electric conductivity are known as promising candidates for smart textiles,[18] non-wetting electromagnetic interference shielding[19] and electrode materials.[20][21] Superhydrophobic/conductive coatings have also found promising applications for microelectronics packaging where they improve the device reliability by avoiding charge accumulation and protection of device against hostile chemical and humid environments.[22] Superhydrophobic/conductive coatings prepared by dispersing carbon based fillers in the hydrophobic matrix of polymer have been extensively reported.[23][24] The use of carbon nanotubes (CNT)[17][18][21][25] and other carbon based materials such as graphene has been vastly explored to fabricate such coatings.[26] Furthermore, the superhydrophobic/conductive coatings prepared by aforementioned reports either do not possess optical transparency or involve high temperature processing or complicated and time consuming processes which are cost intensive. The use of rather inexpensive carbon fillers such as graphite[27][28] and carbon nanofibers (CNF) has not been explored much in comparison to CNT.[29][30] In this study, we report fabrication of superhydrophobic/conductive coatings applying the facile *droplet assisted growth and shaping (DAGS)* method[31] and dip coating which involves application of very low processing temperature (30^{o}C) as compared to those used for coatings prepared with addition of CNT and graphene. The superhydrophobic/conductive coatings are prepared by a combination of silicone nanofilaments (SNF) and CNF. The SNF are prepared by using the DAGS method at room temperature which has advantages such as: (a) no liquid waste production, (b) easy scale-up and (c) processing at ambient temperature and pressure.[13][32][33] Superhydrophobic substrates obtained by the DAGS method are subsequently dip coated in a

suspension of CNF for few minutes to yield electric conductive and superhydrophobic coatings with low sliding angles. Superhydrophobicity, electrical conduction and transparency of the prepared coatings can be tuned by simply controlling the amount of CNF (0.1-1 wt. %) in the suspension. Further, the prepared coatings show good resistance against immersion in water, highly humid and corrosive conditions.

2. Results and Discussion

2.1. Microstructure of CNF coatings

Homogenous and dense growth of SNF was obtained on both sides of the glass substrates after applying the DAGS method. SNF coated substrates were dip coated for 5 minutes in a CNF suspension to fabricate superhydrophobic and conductive coatings. Afterwards substrates were washed with toluene and Milli-Q water followed by drying in nitrogen stream. The schematic of the procedure is shown in **Scheme 1.**

Figure 1a shows the SEM image of *only* SNF coated glass substrate while the inset shows the water contact angle on the coated glass substrate. Figure 1b-c show *hybrid* CNF coatings prepared by dip coating of SNF coated glass substrate in 0.1 and 1 wt. % CNF suspensions, respectively. Insets show water contact angles on corresponding hybrid coatings. SEM images and water contact angles of coatings prepared by dip coating in 0.25, 0.5 and 0.75 wt. % CNF suspensions are shown in Figure S1. SNF when compared to CNF, are significantly smaller in size. Figure 1d shows the size distribution (diameter) of SNF and CNF. Due to the difference in the size of SNF and CNF a distinct difference in the surface morphology of SNF and CNF coatings can be observed by SEM. In addition, compression of the SNF network after dip coating with CNF was observed (Figure 1e-f), which can be attributed to the low stiffness of silicone (SNFs are essentially polysiloxanes) as compared with carbon.[34][35] Even when SNFs are compressed due to dip coating in the CNF suspension they still provide a skeleton for CNF. Figure 1g shows EDX mapping of coatings prepared with 1 wt. % CNF. A clear

indication of presence of CNF on the surface can be observed in elemental mapping, however signals from Si indicate presence of SNF underneath CNF. Due to the presence of CNF the coatings become electrically conductive. The dependence of electrical conductivity (which is expressed in the terms of sheet resistance) as a function CNF content is represented in Figure 2a. The sheet resistance decreases with an increase of the amount of CNF in suspension indicating the increase in electrical conductivity of the coatings (**Figure 2a**). This behavior can be explained by percolation theory. The coatings prepared with different CNF content have different density of CNF at the surface. Electron transport is dependent on conductive pathways (the density of nanofibers in this case). Thus, with the increase of CNF concentration electron transportation is enhanced which in turn reduces the sheet resistance. Interestingly, superhydrophobicity of hybrid coatings also improves with the addition of CNF. An increase in water contact angle and decrease in sliding angle was observed with increasing amount of CNF (Figure 2b). The contact angles increased from $157.7^{o} \pm 1.9^{o}$ (SNF) to $170.4^{o} \pm 1.8^{o}$ (1 wt. % CNF). While the sliding angles decreased from $13.8^{o} \pm 1.6^{o}$ (SNF) to $4.6^{o} \pm 0.91^{o}$ (1 wt. % CNF).

In order to study the effect of the SNF network structure, a control experiment was conducted where the surface functionalization of glass substrates was performed in anhydrous toluene (water below 30 ppm) using trichloroethylsilane. Functionalized glass substrates were dip coated in 1 wt. % CNF suspension and contact angle measurements were performed. The contact angles of glass increased from 0^{o} (superhydrophilic) to $77.9^{o} \pm 3.1^{o}$ (after silane functionalization), while the contact angle values of $91.6^{o} \pm 2.4^{o}$ were observed after dip coating (Figure S2). Dip coating of a bare glass substrate without silane functionalization was also performed but no change in surface wetting was observed (contact angle 0^{o} before and after dip coating). Both control surfaces did not show any electrical conduction after dip coating when samples were tested using 4 probes implying a superhydrophobic skeleton of

SNF is necessary to effectively bind CNF on the substrate to yield superhydrophobic and conductive coatings.

The prepared CNF coatings are not only superhydrophobic and conductive but they also exhibit optical transparency. Figure 2c shows optical photographs of water droplets on hybrid coatings fabricated with 0.1 and 1 wt. % CNF suspension. UV-Vis transmittance spectra of prepared coatings in the wavelength range of 300-900 nm are shown in Figure 2d. Glass substrates coated with SNFs showed higher transmittance (95.4%) as compared with uncoated glass substrates (91.9%) at 550 nm wavelength. The higher transmittance values are because of anti-reflective properties of the prepared SNF.[13][36] Transmittance values of prepared superhydrophobic/conductive hybrid coatings decrease gradually with an increase in the content of CNF in suspension. The value of transmittance decreased from 81.2% (0.1 wt. % CNF) to 41.07% (1 wt. % CNF) at 550 nm wavelength. The decrease in transmittance is related to the light scattering resulting from development of hierarchical structure of CNF with increasing concentration of CNF.[37][38] The literature reports describing fabrication of superhydrophobic, conductive and transparent coatings prepared by the addition of carbonaceous fillers showed the sheet resistance values in the range of 10^6-10^5 Ω/sq.[23][39][40] While in this report the coatings were prepared using very low amounts of CNF (0.1%) exhibited sheet resistance values in the range of 10^5 Ω/sq. Taking into account the time and energy consuming processing used to prepare such coatings as compared to the strategy presented in this report, our technique of fabrication is easy to implement leading to the coatings with better properties.

2.2. Further properties and applications

In addition to electrical conduction the prepared CNF coatings also exhibit self-cleaning ability. **Figure 3a** shows a 5 µL water droplet moving on the surface of hybrid coating (1 wt. % CNF) to remove sand particles. Incorporation of particles in water drop to eventually

clean the surface is clearly visible. The video in SI also shows self-cleaning ability of the prepared hybrid coatings. The snapshots from the video are shown in Figure 3b. Other than self-cleaning property, the prepared coatings exhibit different water adhesion. Within 30 seconds of exposing the surface to water droplet, rolling of droplet was observed for all surfaces. However, after prolong exposure (3-5 minutes) of the surface to water droplet coatings behaved differently. Sticking of droplets was observed for the coatings prepared with SNF or 0.1 wt. % CNF showing strong adhesion of water droplets after prolonged exposure while rolling of droplets after prolonged exposure was observed for the coatings prepared 0.25, 0.5, 0.75 and 1 wt. % CNF. The high and low adhesion of water droplets on the 0.1 wt. % CNF and 1 wt. % CNF coatings is shown in Figure 3c& d. The syringe moving toward the 5 µL water droplet could not remove the droplet from 0.1 wt. % CNF surface. In contrast, the syringe getting in contact with 5 µL water droplet placed on the coating prepared with 1 wt. % CNF could easily remove the water droplet from the surface due to the low adhesion between water droplet and surface. Tuning the adhesion of water can be useful for applications such as droplet transportation and collection.[41][42] Furthermore, surfaces with different adhesive properties can be used for carrying different reactions in confined volumes.[43][44][45] Figure S3 in supporting info shows an example of droplet transportation and collection.

2.3. Stability against different aqueous environments

Environmental conditions often lead to weakening of the superhydrophobic properties of surfaces limiting their practical applications.[22][46][47] The chemical stability of the coatings in acidic or basic conditions as well as preservation of superhydrophobic property of the coatings in humid conditions or water contact is of significant importance. The stability of coatings in humid conditions was measured by placing the substrates in a glass desiccator kept at relative humidity of (90% ± 3%) by flushing humidified nitrogen, while the stability of

coatings against liquid water was tested by dipping the substrates in water. All measurements were performed at room temperature. Substrates prepared with 0.1 and 1 wt. % CNF were used for these measurements. **Figure 4a-b** show contact and sliding angles of the coatings as a function of exposure time to humid atmosphere and water immersion respectively. There was no significant change in the superhydrophobic nature of the coatings even after 16 hours of exposure to humid environment or immersion in water. The coatings also retained their electrical conduction both in humid conditions and water immersion. This illustrates good stability of the prepared superhydrophobic/conductive surfaces in humid environment and water contact.

Usually when surfaces are in contact with acidic or basic fluids degradation in hydrophobicity is observed due to etching.[48] In order to test the long term stability of coatings to acidic or basic fluids, the prepared coatings were immersed into the aqueous solutions of acidic (pH 2) and basic (pH 14) nature. Coatings fabricated with 0.1 wt. % and 1 wt. % CNF were immersed in acidic or basic aqueous solutions up to 7 days and the change in superhydrophobicity was observed by measuring contact and sliding angles of Milli-Q water droplets. **Figure 5a-b** show the contact and sliding angles as function of immersion time in aqueous solutions of pH 2 and pH 14. Coatings immersed in acidic aqueous solutions showed good chemical resistance and behaved superhydrophobic in nature even after 7 days of immersion. A slight decrease in water contact angle was observed for both coatings immersed in acidic aqueous solution. The water sliding angles were affected significantly, i.e. an increase in sliding angle for both coatings was observed. The water sliding angles were below 45^{o} for both surfaces after 7 days of immersion in acidic aqueous solution.

However, in basic conditions contact angle values for both surfaces decreased significantly as a function of immersion time. The sliding angle of $12.16^{o} \pm 2.04^{o}$ was observed for 0.1 wt. % CNF coating after 1 day of immersion in basic conditions (open red circle in Figure 5b). For 0.1 wt. % CNF coating pinning of water droplets was observed after 3, 5 and 7 days of

immersion and droplets did not slide even at inclination of 90°. Sliding of water droplets at 6.6° ± 1° and 7.6° ± 1° was observed for 1 wt. % CNF coatings after 1 and 3 days of immersion in basic conditions (open black squares in Figure 5b). Pinning of droplets was observed for 1 wt. % CNF coatings immersed for longer duration (5 and 7 days). The prepared coatings were quite stable in acidic conditions and the surface morphology was intact, however the etching of the hierarchical structure of CNF was observed after 7 days of immersion in basic conditions (Figure 5c-f).

Superhydrophobic and conductive coatings prepared by the combination of SNF/CNF illustrated better chemical resistance when compared to only SNF coatings at similar conditions. SNF, when immersed in acidic aqueous solution of pH 2 for 7 days, show contact angle values of ~150° and sliding angle values of ~46° (Figure S4a-b). However, in basic aqueous solution of pH 14 the contact angle decreased abruptly and contact angle value of ~25° was observed after 1 day of immersion. A further decrease in contact angle to ~10° was observed after 7 days of immersion in basic aqueous solution indicating complete etching of SNF (Figure S4a & c). CNF coatings exhibit better performance when compared to only SNF coating; especially in basic conditions (pH 14) CNF show good chemical resistance. The prepared CNF coatings exhibit good stability in acidic conditions and retain their microstructure even after 7 days of immersion (Figure 5c & e). However, etching of the fibrous structure after 7 days of immersion in basic conditions can be seen in Figure 5d & f. The extent of etching for 0.1 wt. % CNF coating was more than 1 wt. % CNF which also explains the smaller values of contact angles observed on 0.1 wt. % CNF coatings. The stability of CNF surfaces could be explained by considering the wetting process. We assume a Cassie-Baxter type wetting when the substrates are immersed in aqueous pH solutions.[49] The roughness generated by hierarchical CNF coating causes entrapment of air in the asperities. This in turn reduces the contact area at solid/liquid interface.[50] Only a small fraction of the surface is wetted when the substrate is placed in the aqueous solution delaying corrosion of

the coating. This cushion of air layer was also observed at the surface of substrates when immersed in aqueous pH solutions which retards the degradation of the coatings.

A comparison of the coatings described is made with literature reports involving use of carbon based materials for the fabrication of superhydrophobic/conductive coatings (Table S1). The fabrication of these coatings using the DAGS method and dip coating is very easy to execute and does not involve complex and complicated processing steps and cost intensive equipment. The fabrication of multifunctional coatings involving inexpensive carbon nanofibers using facile processing is an elegant approach. The coatings prepared by this method have optical transparency and show excellent resistance to different environmental conditions such as humidity exposure, water immersion or immersion in corrosive aqueous solutions. The stability against different environmental conditions is superior to the literature reports on coatings involving carbon based fillers (comparison is represented in Supporting Information Table S1).

2.4. Mechanical durability of coatings

In addition to chemical stability, mechanical stability of the coatings is also of significant importance. The mechanical durability of the coatings was checked in terms of their resistance to abrasion. The coatings exhibit low abrasion resistance and loose superhydrophobicity in just 15 abrasion cycles. **Figure 6a** shows contact angle as a function of abrasion cycles for SNF and 1 wt. % CNF coatings. Contact angles decrease sharply as a function of abrasion cycles and loss in superhydrophobicity is observed for both SNF and 1 wt. % CNF. A loss in the surface microstructure of the coatings due to abrasion force can be seen in Figure S5. A loss in the conductive nature of 1 wt. % CNF coatings as a result of abrasion was also observed just after 5 abrasion cycles (substrate was not conductive when tested using 4 probe). The mechanical durability of the coatings can possibly be improved by addition of a polymer. Polymers usually bind effectively with hydrophobic functional groups,

so when the polymer is added it may bind with the hydrophobic network of SNF and improve its mechanical stability. To check this a modified procedure from *Mates et al* was adopted.[29] The details of the procedure can be found in Supporting Information. Parafilm-M (PF) polymer was chosen for this purpose. CNF were added to a PF solution in toluene yielding in a very stable suspension. The coatings prepared containing PF were also superhydrophobic and conductive in nature with very low sliding angles (Figure 6b, Figure S6 & Figure S7), however they lost optical transparency after PF addition. The addition of PF improved the mechanical durability of the coatings. After PF addition the coatings retained superhydrophobicity (contact angle ~150^{o}) up to 35 abrasion cycles (Figure 6c) as compared with the coatings without PF addition (contact angle ~150^{o}) after 15 abrasion cycles (Figure 6a). The coatings prepared with PF also retained their conductive property even after 50 abrasion cycles (Figure 6d). However, the increase in the sheet resistance was observed with increasing number of abrasion cycles, the increase in the sheet resistance could be attributed to the removal of conductive coatings from the surface due to abrasion force. Deterioration of the coatings due to abrasion force was observed when substrates were analyzed under SEM (Figure S9).

3. Conclusion

Superhydrophobic and conductive coatings have been prepared by using energy efficient and time effective techniques. The substrates were coated with superhydrophobic silicone nanofilaments at room temperature by DAGS chemistry which were afterwards dip coated to yield superhydrophobic/conductive coatings. The prepared coatings were transparent to semi-transparent with different adhesion properties which can be used for droplet transportation or droplet confined reactions. The coatings showed self-cleaning ability with good resistance to extreme humid conditions and immersion in water. Further, the coatings exhibit good resistance to corrosive aqueous environments after prolonged immersion. The initially weak

mechanical durability of the prepared coatings was significantly improved by the addition of Parafilm-M. The ability to coat variety of substrates with facile DAGS method followed by quick dip coating can be useful technique for the fabrication of multifunctional superhydrophobic coatings.

4. Experimental Section

Materials and Methods: Microscopic glass slides (26 mm x 76 mm x 0.15 mm) were obtained from Menzel (Braunschweig, Germany). Trichloroethylsilane (TCES, 98%) was purchased from ABCR GmbH (Germany). Carbon nanofibers were purchased from Sigma Aldrich (Switzerland). Deconex solution (11 Universal) was obtained from Borer Chemie (Zuchwill, Switzerland). Parafilm-M® and extra dry toluene were purchased from Sigma Aldrich (Switzerland). $CuSO_4$ was purchased from Sigma Aldrich (Switzerland). All the chemicals were used as received without any further modification. For cleaning purposes Milli-Q water (resistivity 18.2 MΩ.cm at 25°C) was used.

Preparation of substrates: For cleaning substrates were kept in a container filled with 10% v/v aqueous solution of Deconex 11 universal, and were sonicated for 30 min at 30°C. After sonication, the glass slides were washed with Milli-Q water and dried under stream of nitrogen. Activation of substrates was performed in oxygen plasma chamber Femto (Diener Electronics, Nagold Germany) at 100-watt power for 10 minutes at the flow rate of 25 sccm.

Synthesis of silicone nanofilaments by the DAGS method: Synthesis of SNF was performed in a custom-built glass desiccator (6.5 L volume) using literature reported protocol.[13] In short, the pre-cleaned substrates are kept in a desiccator (coating chamber) and the humidity of chamber is adjusted to 35% ± 2% using mixture of dry and humidified nitrogen. The levels of humidity were monitored using EE23 (E+E Elektronik, Germany) hygrometer. After 1 hour of equilibrium, Trichloroethylsilane (3.8 mmol, 0.5 mL) was injected into the glass desiccator

and the substrates were kept at room temperature (~21-22°C) for 4 hours. Finally, a superhydrophobic coating was observed on the substrates.

Preparation of superhydrophobic/conductive surfaces by dip coating: Suspensions of CNF (0.1, 0.25, 0.5, 0.75 and 1 wt. %) in toluene were prepared by sonicating for 15-20 minutes at 30°C. Suspensions of CNF were stable for 10-15 minutes. Hybrid coatings were obtained by dip coating SNF coated substrates in CNF suspension. Dip coating was performed for 5 minutes followed by washing with toluene and Milli-Q water to remove loosely bound CNF. All coated substrates were dried under the stream of nitrogen to remove water and toluene.

Characterization

Scanning electron microscopy: Scanning electron microscopy (SEM) investigation was performed in the Center for Microscopy and Image Analysis (ZMB) of the University of Zurich using Zeiss Supra 50 VP SEM. Prior to SEM analysis, all samples were coated with 10 nm thick platinum layer using Sputter Coater Safematic CCU-010 (Switzerland) under high vacuum. Images were acquired by secondary electron detector with a working distance of 9 mm and accelerating voltage of 6 keV. To calculate size distribution, SEM imaging of CNF deposited on carbon tape and SNF coated glass substrate was performed. At least 150 CNF and SNF were observed using ImageJ® to determine the diameter of nanofibers. JOEL JSM-6010 SEM equipped with energy dispersive x-ray (EDX) detector (Bruker) was used for EDX analysis with an accelerating voltage of 10 keV.

Characterization of superhydrophobicity: For contact angle measurements and self-cleaning investigations contact angle system OCA (Dataphysics, Germany) was used. SCA software (Dataphysics, Germany) was used for contact angle determination. Milli-Q water droplet with a volume of 5 and 10 μL was used for contact angle and sliding angle measurements respectively. For each sample 3-5 contact angle measurements were performed and the average values of contact angles were used for further calculations. Aqueous pH solutions were made using NaOH and HCl. The values of pH were monitored using inoLab® benchtop

pH meter. The stability of surfaces to humid conditions was performed by placing the substrates in the cleaned desiccator kept at relative humidity of 90% ± 3%.

Sheet resistance measurement: Interface 1000 potentiostat (GAMRY Instruments, USA) was used for sheet resistance measurements using 4 probe method. It was used in combination with a custom made kit with four equidistant (5 mm) electrodes. Current in the range of 50-100 µA was applied on outer electrodes and voltage drop on inner electrodes was used to calculate sheet resistance. At least 3 measurements were performed for each sample and an average value of sheet resistance was used for further calculations.

UV/Vis spectroscopy: UV-Vis spectroscopy was performed using Lambda 950 (Perkin Elmer). The sample were scanned in the wavelength range between 300-900 nm with a scan speed of 268 nm/min. The scan interval of 1 nm was used for all samples.

Abrasion resistance: Resistance of functional surfaces to scratch or abrasion was tested using AB5000 Washability Tester (TQC, Netherlands). ASTM standard D4213 for measuring scrub or abrasion resistance of paints and coatings was used to evaluate abrasion resistance of prepared coatings. A sponge with an applied pressure of 1.86 kPa was moved over the substrate with frequency of 5 cycles/min.

Supporting Information

Supporting Information is available from the Wiley Online Library or from the author.

Acknowledgements

We acknowledge the financial support provided by Swiss National Foundation (SNF). We appreciate Dr. Samet Varol for the fruitful discussions and helpful suggestions. Authors are thankful to Felix Donat from the Department of Mechanical Engineering ETH Zurich for his help in arranging 4 probe experiment. We also acknowledge ZMB (University of Zurich) for providing access to their electron microscopic facilities.

Received: ((will be filled in by the editorial staff))
Revised: ((will be filled in by the editorial staff))
Published online: ((will be filled in by the editorial staff))

References

[1] Y. Lu, S. Sathasivam, J. Song, C. R. Crick, C. J. Carmalt, I. P. Parkin, *Science (80-.).* **2015**, *347*, 1132 LP.

[2] K. Chen, Y. Wu, S. Zhou, L. Wu, *Macromol. Rapid Commun.* **2016**, *37*, 463.

[3] F. Guo, Q. Wen, Y. Peng, Z. Guo, *J. Colloid Interface Sci.* **2017**, *494*, 54.

[4] D. Saddiqi, Naeem-ul-Hasan; S. Seeger; Patra, *ChemPhysChem* **2018**.

[5] Y. Lai, Y. Tang, J. Gong, D. Gong, L. Chi, C. Lin, Z. Chen, *J. Mater. Chem.* **2012**, *22*, 7420.

[6] Z. Sun, T. Liao, K. Liu, L. Jiang, J. H. Kim, S. X. Dou, *Small* **2014**, *10*, 3001.

[7] G. B. Hwang, A. Patir, K. Page, Y. Lu, E. Allan, I. P. Parkin, *Nanoscale* **2017**, *9*, 7588.

[8] N. Wang, D. Xiong, Y. Deng, Y. Shi, K. Wang, *ACS Appl. Mater. Interfaces* **2015**, *7*, 6260.

[9] U. Mehmood, F. A. Al-Sulaiman, B. S. Yilbas, B. Salhi, S. H. A. Ahmed, M. K. Hossain, *Sol. Energy Mater. Sol. Cells* **2016**, *157*, 604.

[10] W. L. Min, B. Jiang, P. Jiang, *Adv. Mater.* **2008**, *20*, 3914.

[11] Z. Chu, Y. Feng, S. Seeger, *Angew. Chemie Int. Ed.* **2015**, *54*, 2328.

[12] W. Zhang, Z. Shi, F. Zhang, X. Liu, J. Jin, L. Jiang, *Adv. Mater.* **2013**, *25*, 2071.

[13] G. R. J. Artus, S. Jung, J. Zimmermann, H.-P. Gautschi, K. Marquardt, S. Seeger, *Adv. Mater.* **2006**, *18*, 2758.

[14] I. S. Bayer, A. Biswas, G. Ellialtioglu, *Polym. Compos.* **2011**, *32*, 576.

[15] Z.-T. Li, B. Lin, L.-W. Jiang, E.-C. Lin, J. Chen, S.-J. Zhang, Y.-W. Tang, F.-A. He, D.-H. Li, *Appl. Surf. Sci.* **2018**, *427*, 56.

[16] O. I. Jaakko V. I. Timonen, Mika Latikka, Ludwik Leibler, Robin H. A. Ras, *Science (80-.).* **2013**, *341*, 253.

[17] L. Ye, J. Guan, Z. Li, J. Zhao, C. Ye, J. You, Y. Li, *Langmuir* **2017**, *33*, 1368.

[18] L. Li, Y. Bai, L. Li, S. Wang, T. Zhang, *Adv. Mater.* **2017**, *29*, 1702517.

[19] A. Das, C. M. Megaridis, L. Liu, T. Wang, A. Biswas, *Appl. Phys. Lett.* **2011**, *98*.

[20] J. Zang, S. Ryu, N. Pugno, Q. Wang, Q. Tu, M. J. Buehler, X. Zhao, *Nat. Mater.* **2013**, *12*, 321.

[21] J. Zou, H. Chen, A. Chunder, Y. Yu, Q. Huo, L. Zhai, *Adv. Mater.* **2008**, *20*, 3337.

[22] C. P. Wong, K. S. Moon, In *Nano-Bio- Electronic, Photonic and MEMS Packaging*; 2010; pp. 1–17.

[23] M. Peng, J. Qi, Z. Zhou, Z. Liao, Z. Zhu, H. Guo, *Langmuir* **2010**, *26*, 13062.

[24] J. T. Han, B. K. Kim, J. S. Woo, J. I. Jang, J. Y. Cho, H. J. Jeong, S. Y. Jeong, S. H.

Seo, G.-W. Lee, *ACS Appl. Mater. Interfaces* **2017**, *9*, 7780.

[25] J. Yang, Z. Zhang, X. Men, X. Xu, *Appl. Surf. Sci.* **2009**, *255*, 9244.

[26] H. Hu, Z. Zhao, W. Wan, Y. Gogotsi, J. Qiu, *ACS Appl. Mater. Interfaces* **2014**, *6*, 3242.

[27] I. S. Bayer, V. Caramia, D. Fragouli, F. Spano, R. Cingolani, A. Athanassiou, *J. Mater. Chem.* **2012**, *22*, 2057.

[28] K. Chen, W. Gou, L. Xu, Y. Zhao, *Compos. Sci. Technol.* **2018**, *156*, 177.

[29] J. E. Mates, I. S. Bayer, J. M. Palumbo, P. J. Carroll, C. M. Megaridis, *Nat. Commun.* **2015**, *6*, 8874.

[30] L. Zhu, Y. , Zhang, J. C., Zhai, J. , Zheng, Y. M., Feng, L. and Jiang, *Chem. Eur. J. Chem. Phys.* **2006**, *7*, 336.

[31] G. R. J. Artus, S. Olveira, D. Patra, S. Seeger, *Macromol. Rapid Commun.* **2017**, *38*, 1600558.

[32] G. R. J. Artus, S. Seeger, *Adv. Colloid Interface Sci.* **2014**, *209*, 144.

[33] G. R. J. Artus, S. Seeger, *Ind. Eng. Chem. Res.* **2012**, *51*, 2631.

[34] W. Luheng, D. Tianhuai, W. Peng, *Sensors Actuators A Phys.* **2007**, *135*, 587.

[35] J. C. L. and W. O. and P. H. V. and P. Bergveld, *J. Micromechanics Microengineering* **1997**, *7*, 145.

[36] J. Zhang, S. Seeger, *ChemPhysChem* **2013**, *14*, 1646.

[37] W. Yao, K.-J. Bae, M. Y. Jung, Y.-R. Cho, *J. Colloid Interface Sci.* **2017**, *506*, 429.

[38] F. Wang, X. Wang, A. Xie, Y. Shen, W. Duan, Y. Zhang, J. Li, *Appl. Phys. A Mater. Sci. Process.* **2012**, *106*, 229.

[39] L.-Y. Meng, S.-J. Park, *J. Colloid Interface Sci.* **2010**, *342*, 559.

[40] G.-W. L. Joong Tark Han, Sun Young Kim, Jong Seok Woo, *Adv. Mater.* **2008**, 3724.

[41] X. Su, H. Li, X. Lai, L. Zhang, X. Liao, J. Wang, Z. Chen, J. He, X. Zeng, *ACS Appl. Mater. Interfaces* **2018**, *10*, 4213.

[42] X. Hong, X. Gao, L. Jiang, *J. Am. Chem. Soc.* **2007**, *129*, 1478.

[43] Z. Cheng, M. Du, H. Lai, N. Zhang, K. Sun, *Nanoscale* **2013**, *5*, 2776.

[44] Z. Cheng, R. Hou, Y. Du, H. Lai, K. Fu, N. Zhang, K. Sun, *ACS Appl. Mater. Interfaces* **2013**, *5*, 8753.

[45] A. Küchler, M. Yoshimoto, S. Luginbühl, F. Mavelli, P. Walde, *Nat. Nanotechnol.* **2016**, *11*, 409.

[46] L. Feng, Z. Yang, J. Zhai, Y. Song, B. Liu, Y. Ma, Z. Yang, L. Jiang, D. Zhu, *Angew. Chemie - Int. Ed.* **2003**, *42*, 4217.

[47] Y. Zhu, J. Zhang, Y. Zheng, Z. Huang, L. Feng, L. Jiang, *Adv. Funct. Mater.* **2006**, *16*, 568.

[48] J. Zimmermann, G. R. J. Artus, S. Seeger, *Appl. Surf. Sci.* **2007**, *253*, 5972.

[49] A. B. D. Cassie, S. Baxter, *Trans. Faraday Soc.* **1944**, *40*, 546.

[50] D. Quére, A. Lafuma, J. Bico, *Nanotechnology* **2003**, *14*, 1109.

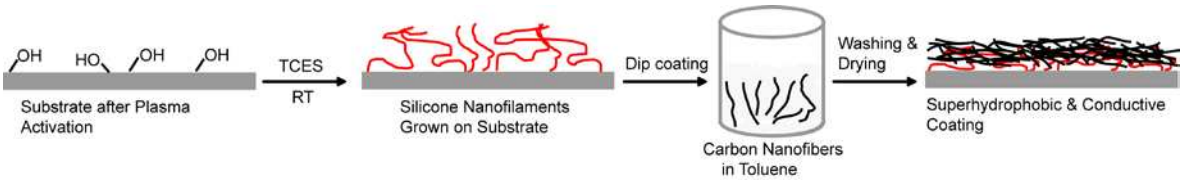

Scheme 1. Activation of substrates to create (-OH) moieties followed synthesis of SNF using trichloroethylsilane (TCES) at room temperature. Dip coating of SNF substrates in CNF suspension to fabricate hybrid CNF surfaces

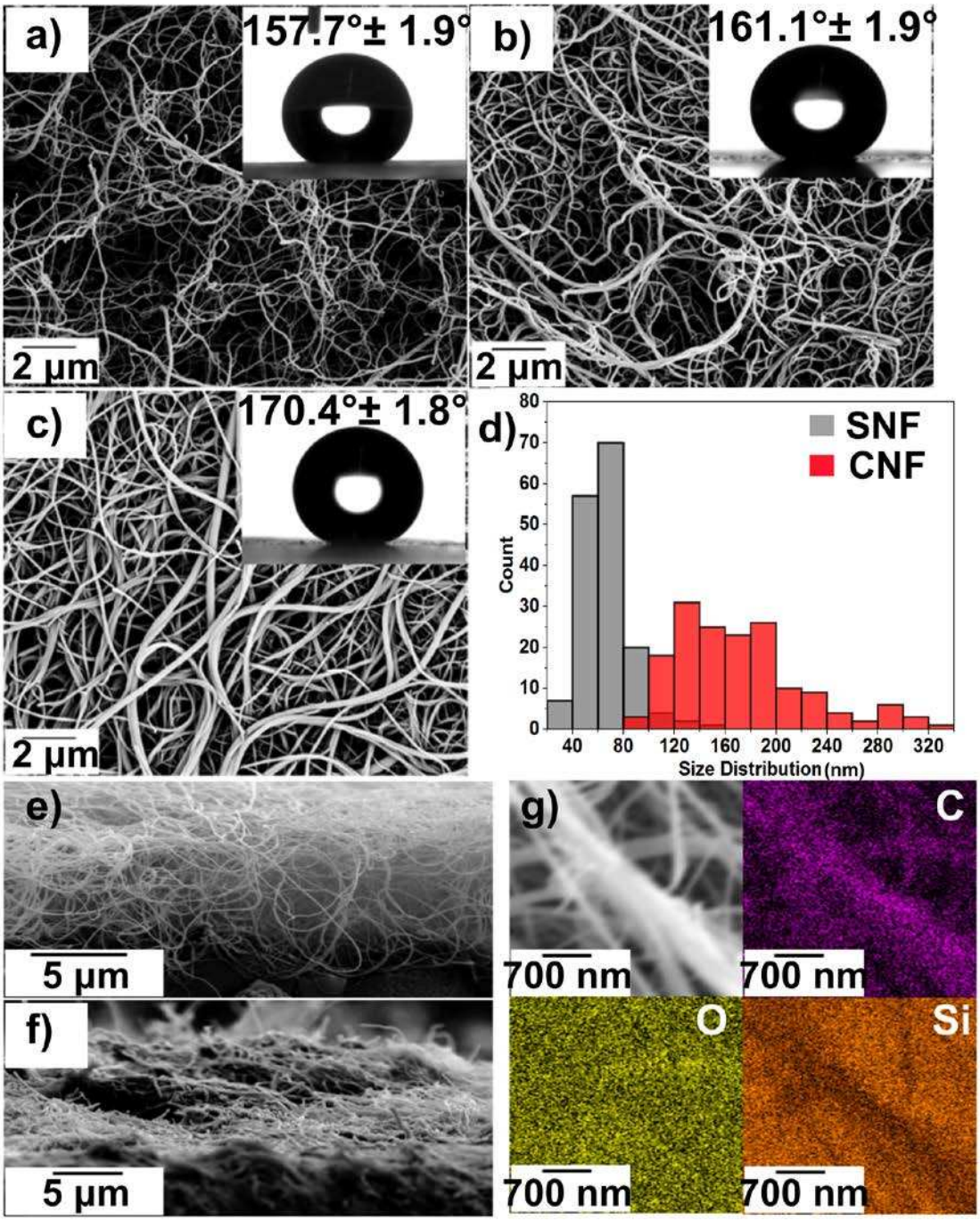

Figure 1. SEM of (a) SNF coated glass substrate, (b) 0.1 and (c) 1 wt. % CNF coatings, and insets show water contact angles, (d) size distribution of SNF and CNF, cross-sectional view (e) SNF, (f) 1 wt. % CNF coatings, (g) SEM image and elemental mapping on 1 wt. % CNF coatings

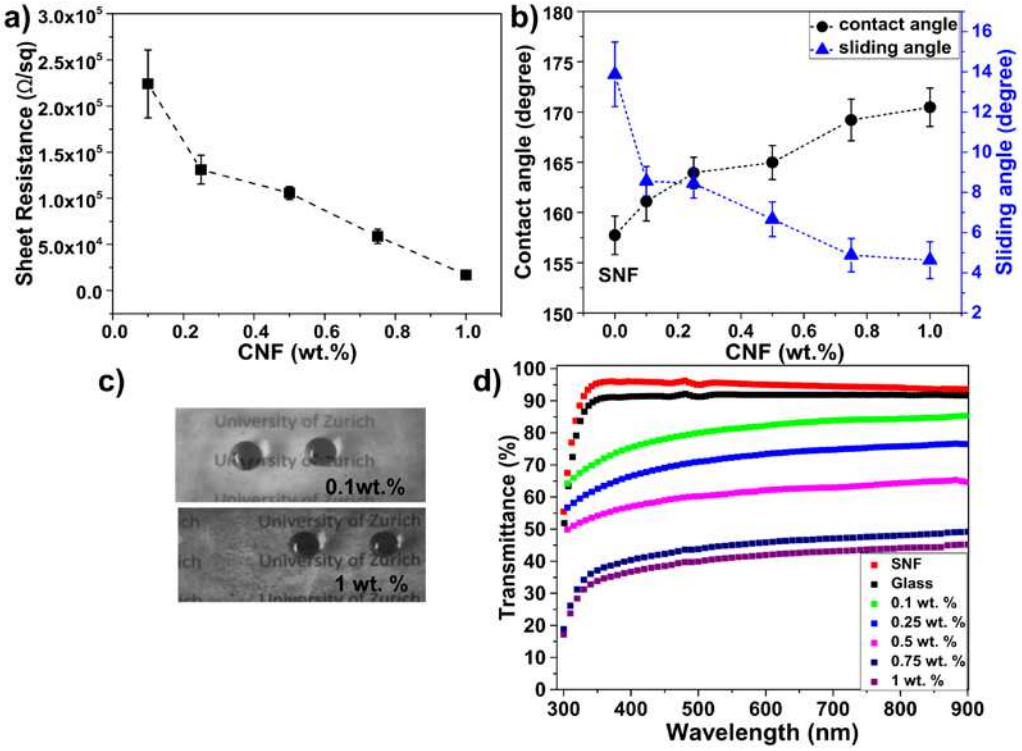

Figure 2. Sheet resistance (a), contact and sliding angles (b) as a function of CNF content, (c) optical photographs and (d) transmittance spectra of coatings fabricated with different concentration of CNF

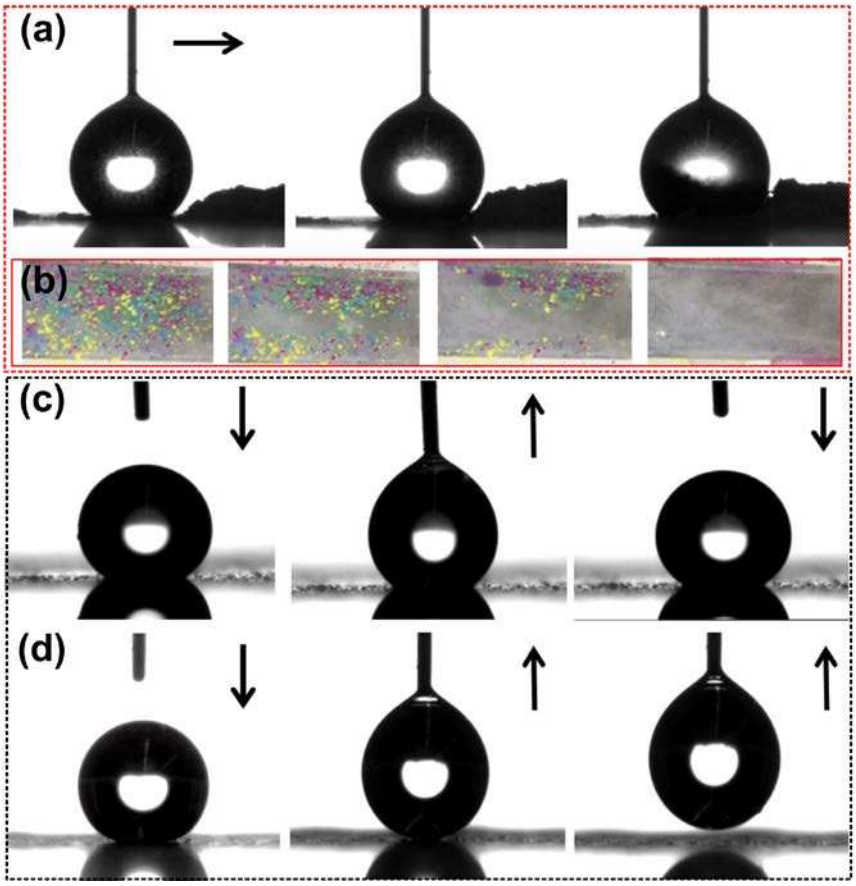

Figure 3. (a) Self-cleaning ability of surface fabricated with 1 wt. % CNF using 5 µL water droplet, surface is covered with sand particles, (b) photographs showing removal of chalk particles from the surface with stream of water (images are snapshots of the video showing self-cleaning property), (c) 5 µL water droplet sticking to the surface prepared with 0.1 wt. % CNF and (d) syringe moves to make contact with 5 µL water droplet, the droplet is suspended from the syringe when it departs the surface prepared by 1 wt. % CNF. The arrows indicate the direction of syringe movement

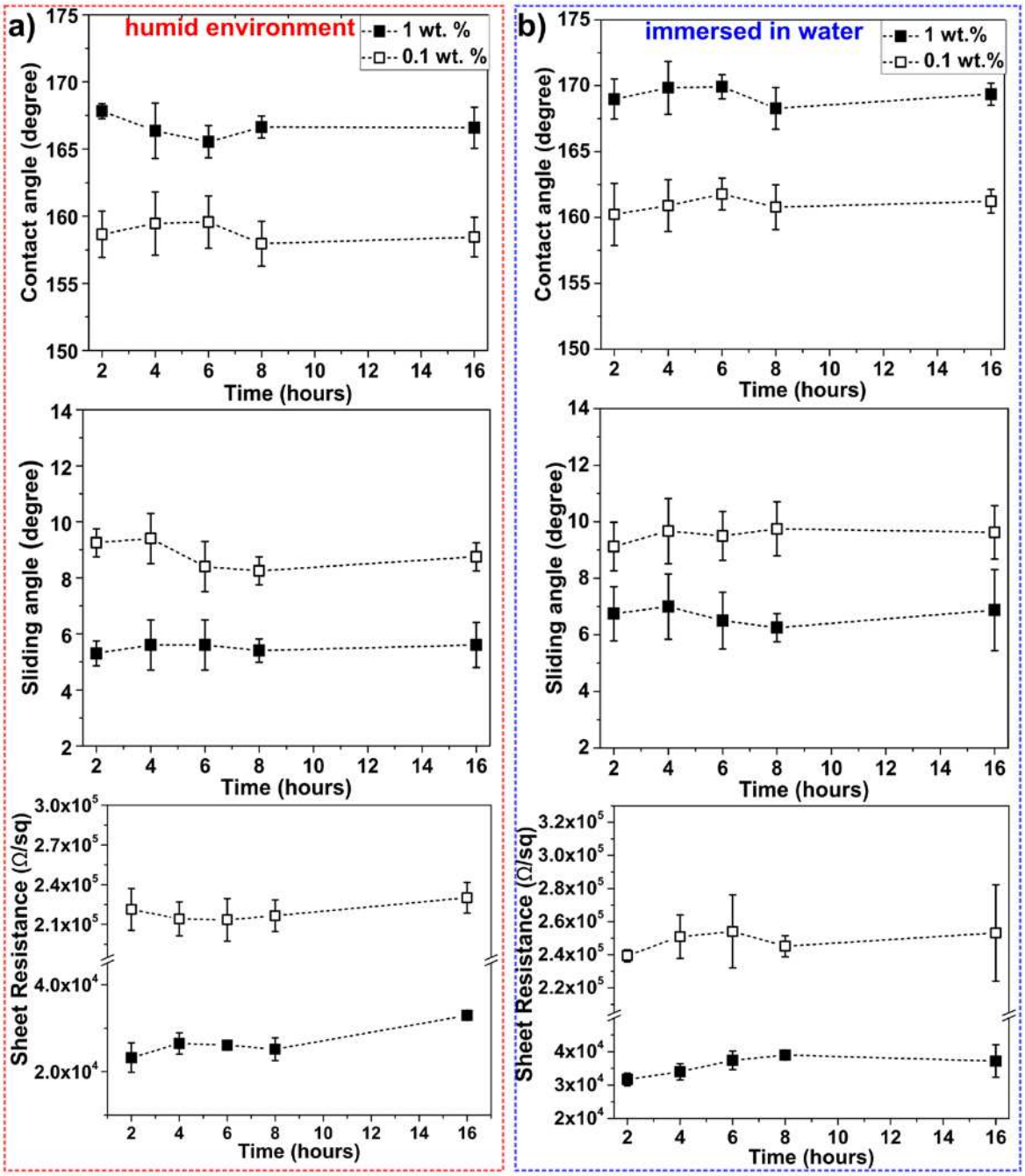

Figure 4. Contact angles, sliding angles and sheet resistance of 0.1 & 1 wt. % CNF coatings exposed to (a) humid conditions and (b) water immersion

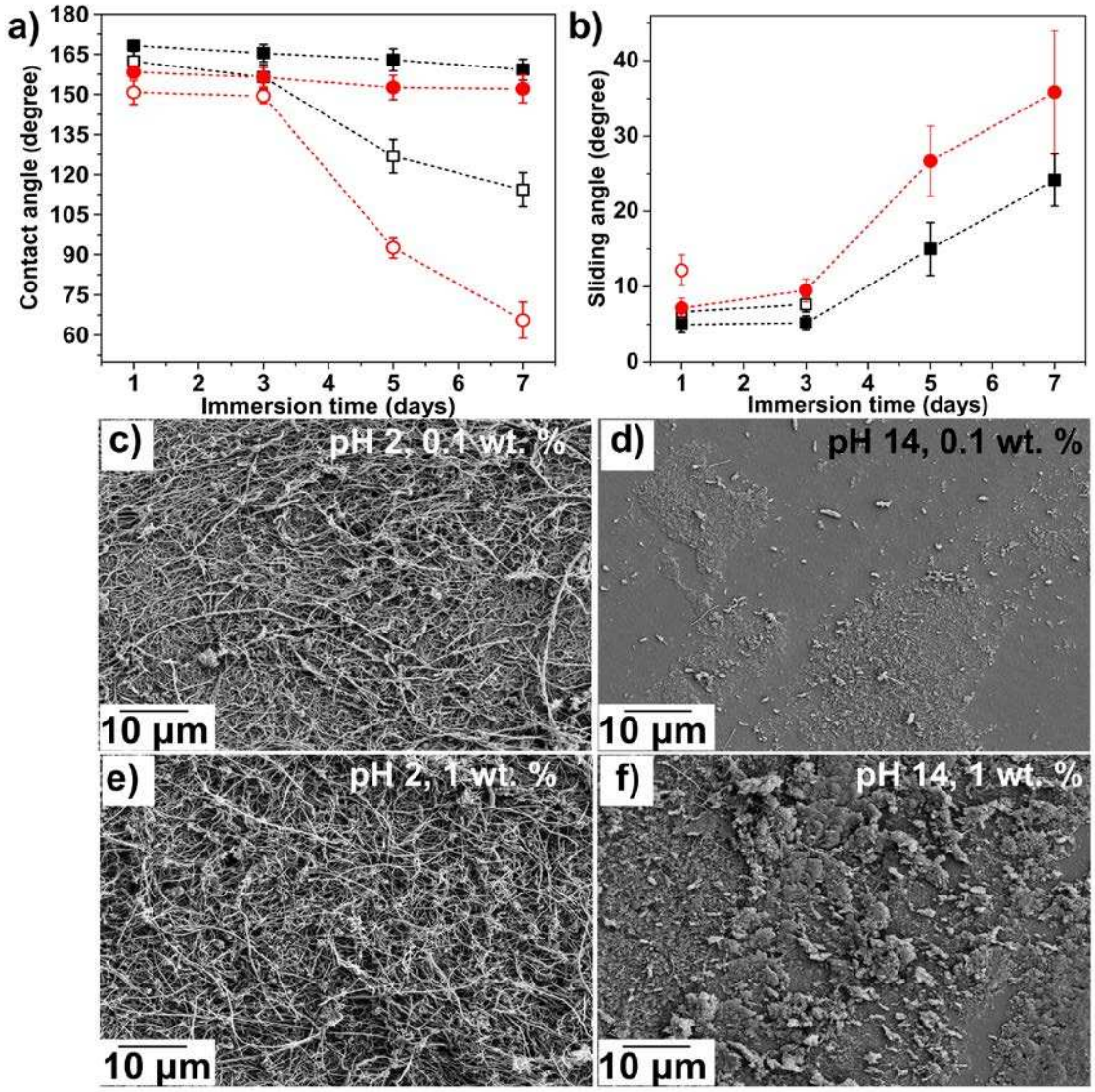

Figure 5. (a) Contact angles, (b) sliding angles as a function of immersion time in aqueous pH solutions (1 wt. % CNF in ■ pH 2 & □ pH 14, 0.1 wt. % CNF in ● pH 2 & ○ pH 14), SEM of 0.1 wt. % CNF coating after 7 days of immersion in (c) pH 2 and (d) pH 14, SEM of 1 wt. % CNF coating after 7 days of immersion in (e) pH 2 and (f) pH 14 aqueous solutions

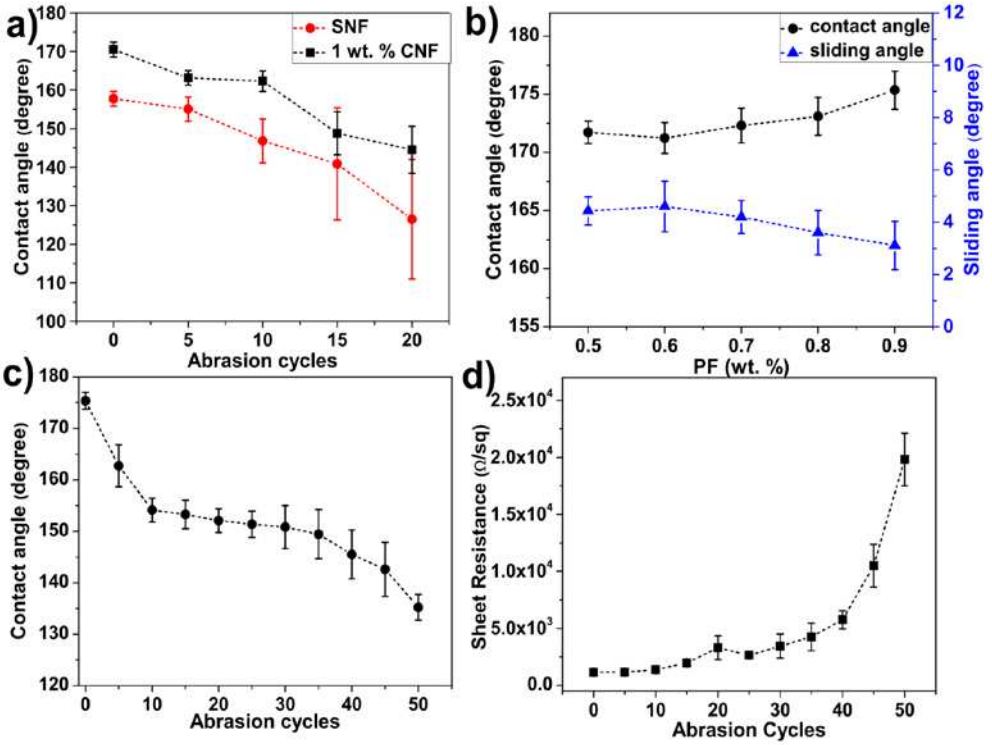

Figure 6. (a) Contact angles of SNF and 1 wt. % coatings as a function of abrasion cycles, (b) contact and sliding angles as a function of PF content in the suspension, (c-d) contact angle and sheet resistance of the coatings prepared with 0.9 wt. % PF addition as a function of abrasion cycles

The table of contents entry

Fabrication of multifunctional superhydrophobic & conductive coatings by applying a facile method is presented in this report. Silicone nanofilaments and carbon nanofibers have been used to create such coatings which possess tunable transparency and excellent resistance to extreme environmental conditions and corrosive liquids.

Keyword: Silicone nanofilaments, superhydrophobic coatings, droplet assisted growth and shaping, electrically conductive coatings, carbon nanofibers

N. H. Saddiqi, S. Seeger*

Chemically Resistant, Electric Conductive & Superhydrophobic Coatings

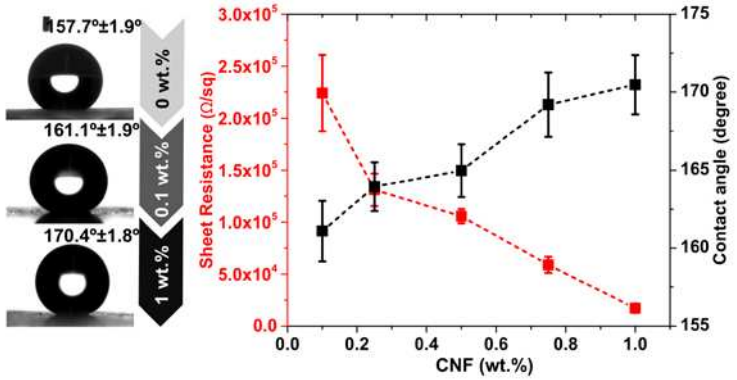

Supporting Information

Chemically Resistant, Electric Conductive & Superhydrophobic Coatings

*Naeem-ul-Hasan Saddiqi, Stefan Seeger**

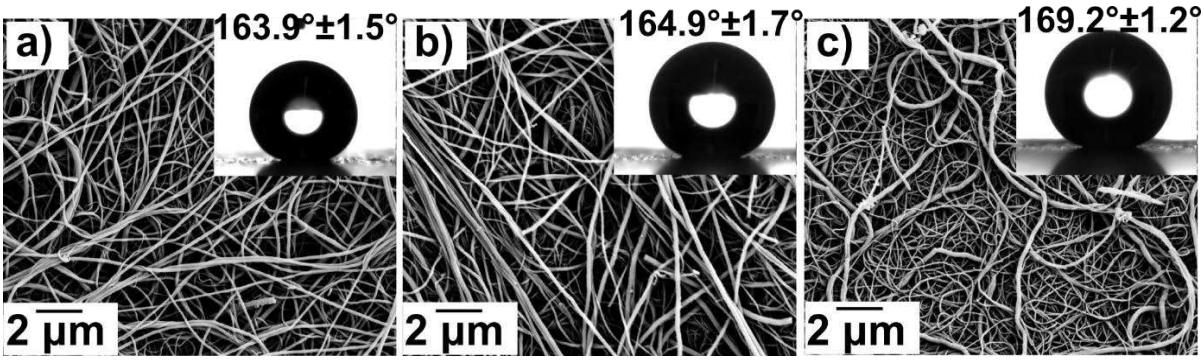

Figure S1. SEM of (a) 0.25, (b) 0.5 and (c) 0.75 wt. % CNF coatings. Water contact angles are shown in insets

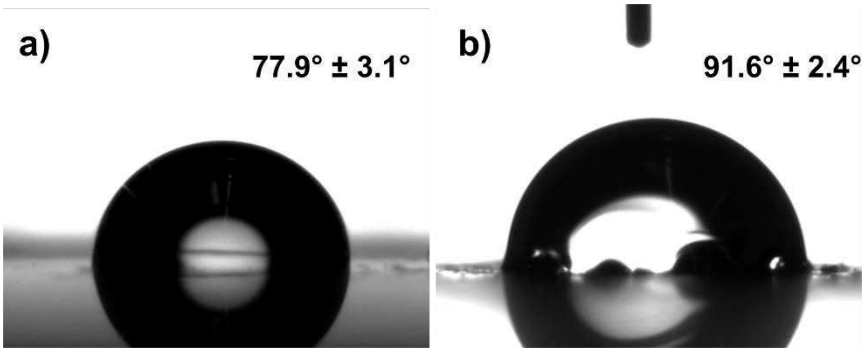

Figure S2. Contact angle (a) glass substrate after silane functionalization, and (b) silane functionalized glass substrate after dip coating

Droplet transportation

To show droplet transportation and droplet confined reaction a very common reaction between $CuSO_4$ and NaOH has been selected for demonstration purpose. Aqueous solutions of 0.1 M $CuSO_4$ and 0.2 M NaOH were prepared. The $CuSO_4$ solution was placed on the surface with low adhesion (1 wt. % CNF), while the aqueous solution of NaOH was deposited on the surface with high adhesion (0.1 wt. % CNF). The droplet containing $CuSO_4$ could be easily transported from low adhesion surface with a metal tip (Figure S3a-d) to high adhesion surface (Figure S3e). After merging of two droplets precipitates of $Cu(OH)_2$ were formed (Figure S3g-h) due to the reaction between Cu^{2+} and OH^-. It is just one example of the

possible use of surfaces with varying adhesion properties, therefore further characterization of the species formed inside the water droplet after coalescence of two droplets was not made.

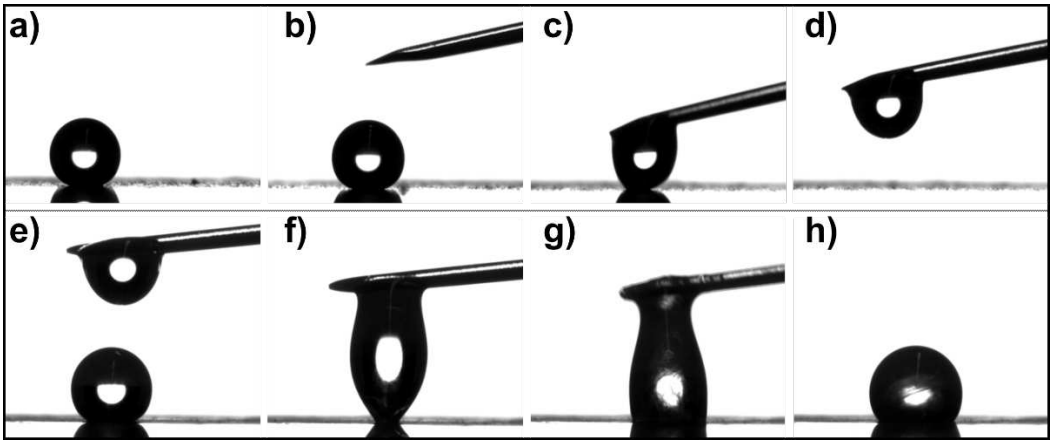

Figure S3. (a-d) Water droplet containing $CuSO_4$ is transferred from low adhesive surface with the metal tip, (e) water droplet containing NaOH is placed on the surface with high adhesion, while the metal tip containing $CuSO_4$, (f) merging of two droplets and (g-h) formation of flocculent.

Chemical stability

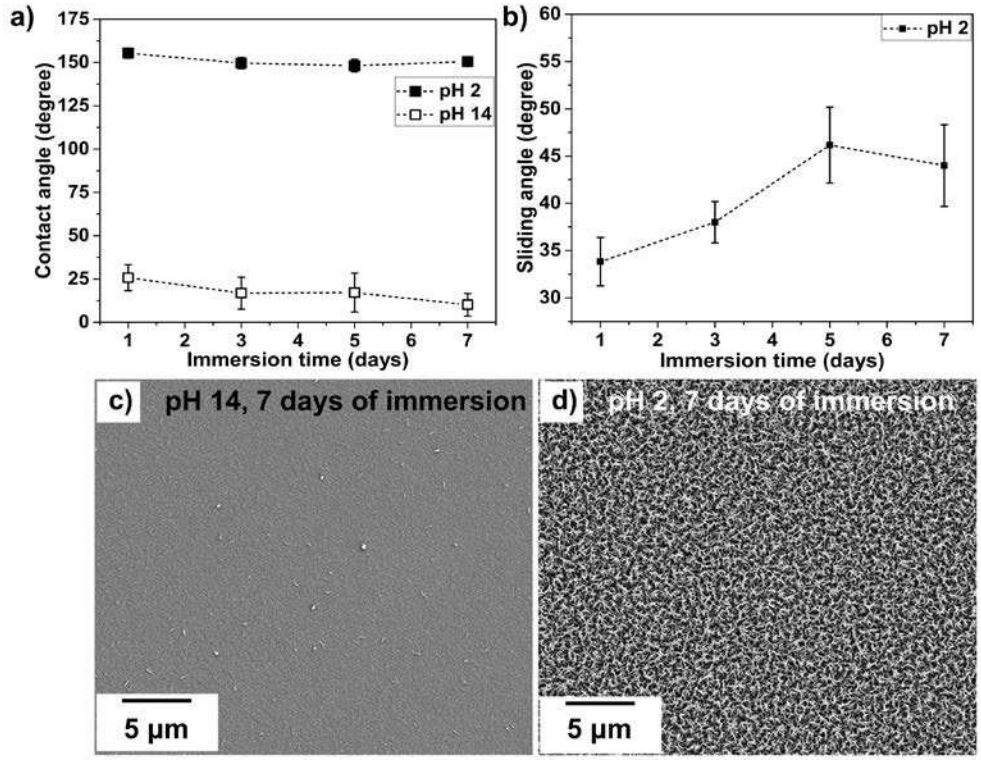

Figure S4. (a) Contact angle, (b) sliding angle on SNF coated substrates as a function of immersion time in aqueous solutions of pH 2 and pH 14, SEM image of SNF coated substrate after 7 days of immersion in (c) pH 14 and (d) pH 2 aqueous solution

Table S1. Comparison of our work with the literature reports involving carbonaceous materials for the fabrication of superhydrophobic/conductive coatings

Materials	**Processing conditions (method[1], temperature[2], duration[3])**	**Transparency**	**Chemical resistance**		**Reference**
			Water immersion/humid conditions	**Acidic and basic conditions**	
CNF	Dip coating, 30ºC, ~5 hours	Fully to semi-transparent	- Stable to water immersion (16 hours) - Stable in humid conditions (16 hours)	- Stable to acidic solutions (~7 days) - Stable to basic solutions (~3 days)	This work
CNF	Spray coating, 75ºC, 24 hours	Not reported	Not reported	Not reported	[1]
CNF	Spray coating, 90ºC	Not reported	Not reported	Not reported	[2],[3]
Graphite	Spray coating, room temperature, >1 hour	Non-transparent	Not reported	Stable to acidic and basic solutions (~ 24 hours)	[4]
Graphite	Drop casting, 350ºC	Not reported	Not reported	Not reported	[5]
Carbon nanocapsules	Dip coating, 120ºC, ~4 hours	Not reported	Stable in humid conditions (2 hours)	- Stable to acidic solution (~ 2 hours) - Stable to basic solutions (~ few minutes)	[6]
Carbon black	Powder treatment & pellet making, 25-200ºC, >24 hours	Not reported	Not reported	Not reported	[7]
Ketjen black, Graphene, CNT	Molding, >100ºC	Not reported	Not reported	Not reported	[8]
Graphene	Polymer infiltration, 120ºC, ~12 hours	Not reported	Not reported	Not reported	[9]
MWCNT	Filtration, 40ºC, ~12 hours	Not reported	Not reported	Stable to acidic and basic solutions (~ few minutes)	[10]
MWCNT	Screen printing, 250ºC	Not reported	Not reported	Not reported	[11]

[1] Method used for fabrication of superhydrophobic/conductive materials
[2] Indicates maximum processing temperature used, it does not include the temperature used for the synthesis of carbonaceous fillers
[3] Indicates total duration for fabrication of superhydrophobic/conductive materials. Does not include the time for the synthesis of carbonaceous fillers

MWCNT	Spray coating, 210ºC	Fully to semi-transparent	Not reported	Not reported	[12]
MWCNT	Dip coating, 70ºC, ~90 hours	Fully to semi-transparent	Not reported	Not reported	[13]
MWCNT	Filtration, 60-80ºC, ~24 hours	Not reported	Not reported	Not reported	[14]
MWCNT	Spray coating, 125ºC, >72 hours	Transparent	Not reported	Not reported	[15]
MWCNT	Polymer infiltration, 190ºC	Not reported	- Stable to water immersion (25 hours)	Not reported	[16]
MWCNT	Drop casting, ~80ºC, ~72 hours	Not reported	Not reported	Not reported	[17]
MWCNT	Spray coating, 60ºC, ~48 hours	Non-transparent	Not reported	Not reported	[18]
MWCNT	Spray coating, >60ºC, >65 hours	Fully to semi-transparent	Not reported	Not reported	[19]
MWCNT	Spray coating, room temperature, ~24 hours	Fully to semi-transparent	Not reported	Not reported	[20]
MWCNT	Free radical polymerization, >50ºC, >48 hours	Not reported	Not reported	Stable to acidic and basic solutions (210 days)	[21]
MWCNT	Micro laser texturing, 80ºC, 3 hours	Not reported	Not reported	Not reported	[22]

The comparison of processing conditions and properties of the coatings presented in this study is made with literature studies which involve application of carbon based materials for the fabrication of superhydrophobic/conductive coatings (Table S1). The superhydrophobic/conductive coatings reported in this work are easy to fabricate in terms of the ease in processing, instrumentation used and processing temperatures. Further, the coatings exhibit better performance in different environmental conditions when compared to the literature reports which involve the use of carbonaceous filler materials for the fabrication of superhydrophobic/conductive coatings.

Mechanical durability of coatings

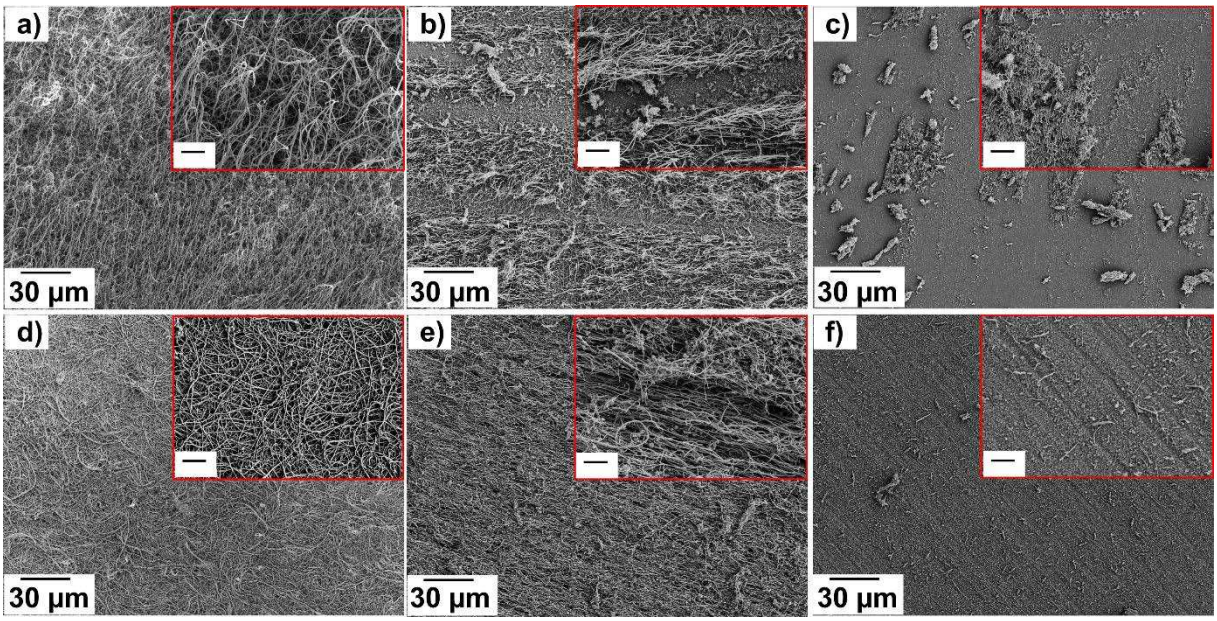

Figure S5. SEM of SNF coated substrates after (a) 0, (b) 5 and (c) 20 abrasion cycles. 1 wt. % CNF substrates after (d) 0, (e) 5 and (f) 20 abrasion cycles. The scale bar of insets is 5 µm

Coatings prepared with Parafilm-M addition

The procedure used was modification of method reported by Mates et al.[1] Parafilm-M (PF) was dissolved in toluene at 50ºC under continuous stirring for 30 minutes. The prepared PF solution was added to CNF dispersion in toluene to yield *x* wt. % PF+1 wt. % CNF dispersions. Solutions with varying concentration of PF in toluene were prepared. For this purpose 0.125, 0.15, 0.175, 0.2 and 0.225 g of PF was dissolved in 5 ml of toluene and added in CNF dispersion to yield 0.5, 0.6, 0.7, 0.8 and 0.9 wt. % PF in final solution. Sonication for 10 minutes was performed to obtain a stable dispersion. The dispersion were stable for several weeks. Afterwards, SNF coated glass substrates were dip coated in the prepared dispersions for 5 minutes. Washing of the substrates in toluene and water was performed followed by drying in the nitrogen stream. The prepared substrates were characterized by SEM. Figure S6 shows the SEM images of the coatings prepared with varying PF content. Agglomerated and

aggregated structures of the polymer/CNF were observed with increasing amount of PF in the dispersion. The coating prepared were superhydrophobic and conductive in nature. Interestingly decrease in the sheet resistance and an increase in the hydrophobicity of the prepared coatings due to the addition of PF was observed (Figure S7). The decrease in the sheet resistance with the increase in PF content can be attributed to the good binding of CNF to SNF due to the presence of PF polymer and increase in the overall thickness of the prepared coatings. The increase in the thickness of the coating prepared with 0.9 wt. % PF can be seen in Figure S8. The thickness of the coating prepared with PF addition is higher than SNF and 1 wt. % CNF/SNF (Figure 1f). The fabrication of thick coatings after dip coating SNF coated substrate in PF+CNF dispersions results in the increased conductivity (or decreased sheet resistance). The coatings prepared with PF addition were not transparent in nature.

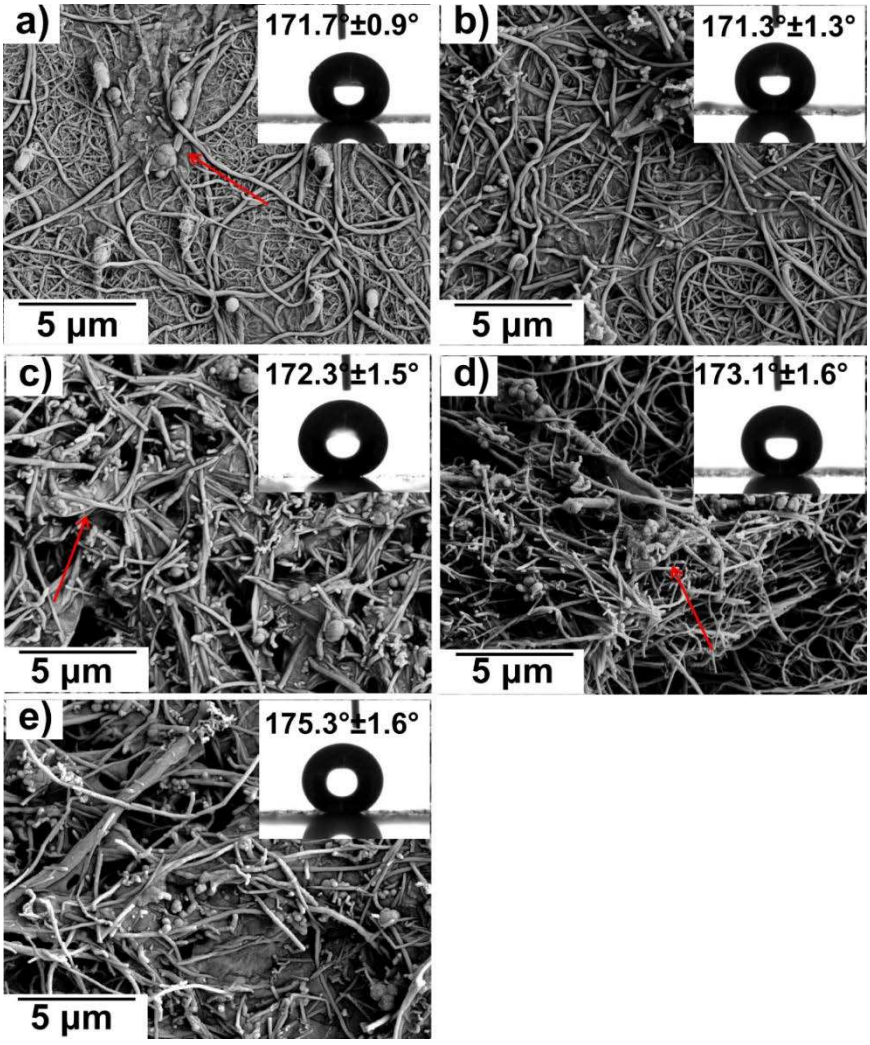

Figure S6. SEM of coatings prepared with (a) 0.5, (b) 0.6, (c) 0.7, (d) 0.8 and (e) 0.9 wt. % PF in 1 wt. % CNF dispersion. Insets show the contact angles of water droplets on corresponding surfaces. Some aggregated structures were also observed due to PF addition. The red arrows show formation of aggregated structures

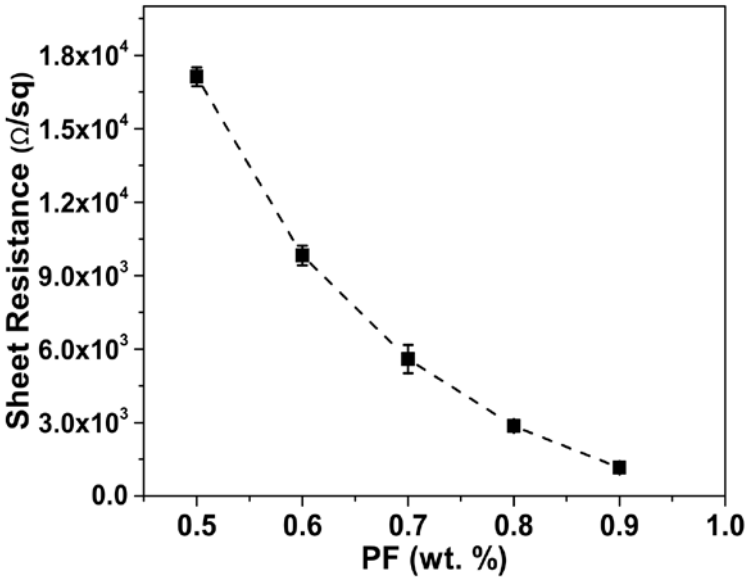

Figure S7. Sheet resistance as a function of PF addition

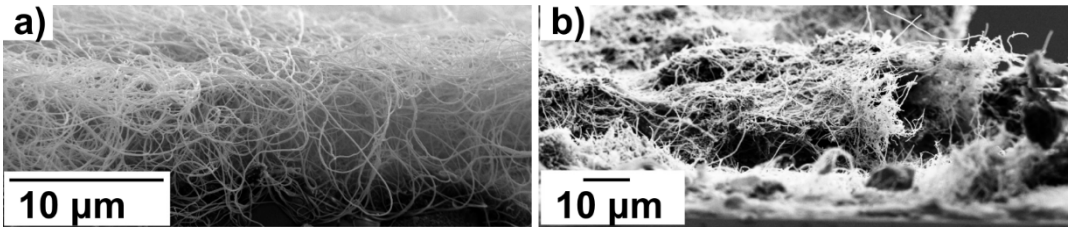

Figure S8. Cross-sectional view of (a) SNF coating and (b) coating prepared with 0.9 wt. % PF addition

To check the mechanical stability coatings prepared with highest PF content (0.9 wt. %) were used. Due to the good binding ability of PF polymer blend the mechanical performance of the coatings was improved. The coatings were superhydrophobic in nature even up to 35 abrasion cycles. With the increase in the number of abrasion cycles deterioration of the surface structure was observed (as indicated with red lines in Figure S9). Given the fact very small amount of PF was used for fabrication of such coatings, the mechanical performance of the coatings may improve if high concentration of PF is used.

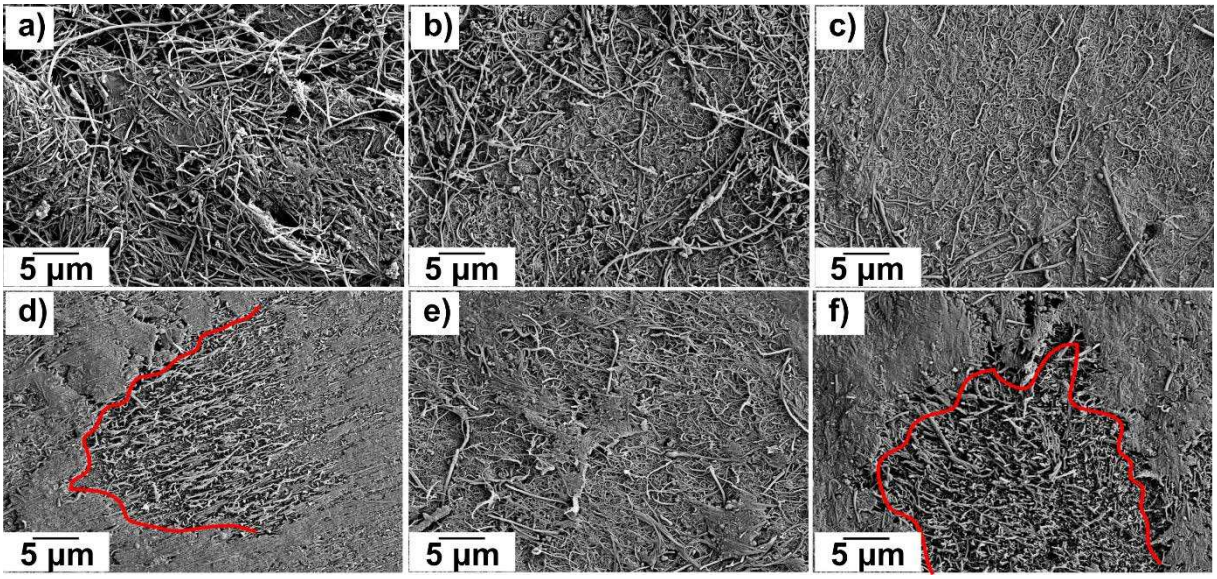

Figure S9. SEM of coatings prepared with 0.9 wt. % PF addition after (a) 0, (b) 10, (c) 20, (d) 30, (e) 40, and (f) 50 abrasion cycles. Regions marked red show the abrasion of the coatings

References

[1] J. E. Mates, I. S. Bayer, J. M. Palumbo, P. J. Carroll, C. M. Megaridis, *Nat. Commun.* **2015**, *6*, 8874.

[2] A. Das, H. T. Hayvaci, M. K. Tiwari, I. S. Bayer, D. Erricolo, C. M. Megaridis, *J. Colloid Interface Sci.* **2011**, *353*, 311.

[3] A. Das, T. M. Schutzius, I. S. Bayer, C. M. Megaridis, *Carbon N. Y.* **2012**, *50*, 1346.

[4] K. Chen, W. Gou, L. Xu, Y. Zhao, *Compos. Sci. Technol.* **2018**, *156*, 177.

[5] I. S. Bayer, V. Caramia, D. Fragouli, F. Spano, R. Cingolani, A. Athanassiou, *J. Mater. Chem.* **2012**, *22*, 2057.

[6] N. Mittal, D. Deva, R. Kumar, A. Sharma, *Carbon N. Y.* **2015**, *93*, 492.

[7] M. Sansotera, W. Navarrini, G. Resnati, P. Metrangolo, A. Famulari, C. L. Bianchi, P. A. Guarda, *Carbon N. Y.* **2010**, *48*, 4382.

[8] L. Shen, H. Ding, Q. Cao, W. Jia, W. Wang, Q. Guo, *Carbon N. Y.* **2012**, *50*, 4284.

[9] H. Hu, Z. Zhao, W. Wan, Y. Gogotsi, J. Qiu, *ACS Appl. Mater. Interfaces* **2014**, *6*, 3242.

[10] L. Ye, J. Guan, Z. Li, J. Zhao, C. Ye, J. You, Y. Li, *Langmuir* **2017**, *33*, 1368.

[11] J. T. Han, B. K. Kim, J. S. Woo, J. I. Jang, J. Y. Cho, H. J. Jeong, S. Y. Jeong, S. H. Seo, G.-W. Lee, *ACS Appl. Mater. Interfaces* **2017**, *9*, 7780.

[12] M. Peng, J. Qi, Z. Zhou, Z. Liao, Z. Zhu, H. Guo, *Langmuir* **2010**, *26*, 13062.

[13] L.-Y. Meng, S.-J. Park, *J. Colloid Interface Sci.* **2010**, *342*, 559.

[14] H. Yao, C.-C. Chu, H.-J. Sue, R. Nishimura, *Carbon N. Y.* **2013**, *53*, 366.

[15] J. Yang, Z. Zhang, X. Men, X. Xu, *Appl. Surf. Sci.* **2009**, *255*, 9244.

[16] M. Peng, Z. Liao, J. Qi, Z. Zhou, *Langmuir* **2010**, *26*, 13572.

[17] J. Zou, H. Chen, A. Chunder, Y. Yu, Q. Huo, L. Zhai, *Adv. Mater.* **2008**, *20*, 3337.

[18] F. Zhang, H. Qian, L. Wang, Z. Wang, C. Du, X. Li, D. Zhang, *Surf. Coatings Technol.* **2018**, *341*, 15.

[19] G.-W. L. Joong Tark Han, Sun Young Kim, Jong Seok Woo, *Adv. Mater.* **2008**, 3724.

[20] W. Yao, K.-J. Bae, M. Y. Jung, Y.-R. Cho, *J. Colloid Interface Sci.* **2017**, *506*, 429.

[21] L. Zhao, W. L. Liu, L. D. Zhang, J. S. Yao, W. H. Xu, X. Q. Wang, Y. Z. Wu, *Colloids Surfaces A Physicochem. Eng. Asp.* **2013**, *423*, 69.

[22] P. O. Caffrey, M. C. Gupta, *Appl. Surf. Sci.* **2014**, *314*, 40.